Available online at www.sciencedirect.com
SCIENCE DIRECT®
International Journal of Heat and Fluid Flow 25 (2004) 671–682
International Journal of HEAT AND FLUID FLOW
www.elsevier.com/locate/ijhff

Correlation for Nusselt number in natural convection in vertical convergent channels at uniform wall temperature by a numerical investigation

A.S. Kaiser *, B. Zamora, A. Viedma

Dpto. Ingeniería Térmica y de Fluidos, Universidad Politécnica de Cartagena, Doctor Fleming s/n, 30202 Cartagena, Spain

Received 30 April 2003; accepted 11 November 2003
Available online 1 February 2004

Abstract

A numerical study of natural convective flows in a vertical converging channel for different angles of convergence has been carried out, taking into account the lacks reported in the literature on some aspects of this configuration. Two-dimensional laminar simulations were obtained by solving the fully elliptic governing equations using two different general purpose codes: Fluent and Phoenics. Special emphasis is made on the systematic comparisons of computational results with experimental and numerical data taken from literature. A generalized correlation for the average Nusselt number has been obtained from numerical results in a channel with isothermal heated plates, for symmetric and asymmetric heating conditions. This correlation has been obtained for wide and not yet covered ranges of the modified Rayleigh number varying from 1 to 10^6 and the angle of convergence from 1° to 30°. Good agreement has been obtained with respect to the available experimental asymptotes of the bibliography for fully developed and boundary layer regimes.

Keywords: Convective flows; Converging channels; Numerical correlation

1. Introduction

Natural convection processes are widely used in thermal control of many systems because of its cheapness, easy maintenance and reliability. Common applications include the cooling of electronic equipment and nuclear reactors, heat exchangers, building industry (solar chimneys and Trombe walls) and many others fields. Typically, these channels are open to ambient conditions at both the inlet and the outlet sections. For an efficient behaviour of natural convection in cooling processes it is advisable to fully understand the heat dissipation phenomena at different geometrical configurations. However, most investigations have treated severely idealised situations.

A great number of analytical, numerical, and experimental works have been carried out on this problem since Elenbaas (1942) first introduced the problem of natural convection between parallel vertical plates. Bodoia and Osterle (1962) reported the first numerical solution for developing flow between plates at uniform wall temperature. More recently, Manca et al. (2000) have reported a useful review on this configuration. Guo and Wu (1993) have systematically studied the variable property effects on the air flow induced by natural convection in vertical channels in symmetrically heated channels. Influence of variable properties effects on flows in asymmetrically heated vertical channels was investigated by Zamora and Hernández (1997).

Numerical and experimental results for an inclined heated channel were obtained by Straatman et al. (1994) and Bianco et al. (2000). Baskaya et al. (1999) studied the asymmetric natural convection heat transfer for this configuration. However, the study of natural convection flows in configurations including sloped (and no-parallel) walls has received only a limited attention. Many applications such as solar chimneys and Trombe walls include structures based on converging channels

* Corresponding author. Tel.: +34-968-325-984; fax: +34-968-325-999.
E-mail address: antonio.kaiser@upct.es (A.S. Kaiser).

0142-727X/$ - see front matter © 2003 Elsevier Inc. All rights reserved.
doi:10.1016/j.ijheatfluidflow.2003.11.022

Nomenclature

$\mathscr{A}$, $\mathscr{B}$	constants in Eq. (12)
b	minimum inter-plate spacing in the converging channel (Fig. 1)
c_p	specific heat at constant pressure
g	gravitational acceleration
Gr	Grashof number, $g\beta(T_w - T_\infty)(\cos\gamma)b^3/v_\infty^2$
h	heat transfer coefficient, $(Nu)\kappa/b$
L	streamwise length of wall (Fig. 1)
n	correlation exponent in Eq. (8)
Nu	average Nusselt number, Eq. (7)
Nu_χ	local Nusselt number, $h\chi/\kappa$
p	pressure
p'	reduced pressure $p' = p - p_\infty$
Pr	Prandtl number, $\mu_\infty c_{p,\infty}/\kappa_\infty$
Ra	Rayleigh number, $(Gr)(Pr)$
Ra^*	modified Rayleigh number, $Ra(b/L)$
T	temperature
T_w	wall temperature
T_∞	ambient temperature
u, v	velocity components in the x and y directions
$\vec{v}$	velocity vector
x, y	cartesian coordinates (Fig. 1)

Greeks

β	coefficient of thermal expansion, $1/T_\infty$
γ	inclination or converging angle (Fig. 1)
κ	thermal conductivity
Λ	coefficient in Eq. (10)
μ	viscosity
v	kinematic viscosity
ρ	density
χ	coordinate along the wall (Fig. 1)

Subscripts

bl	boundary-layer limit
fd	fully developed limit
max	maximum inter-plate spacing
r	reference conditions
∞	ambient conditions

(interest in passive solar heating has increased significantly over the last years and will continue). Sparrow et al. (1988), and Sparrow and Ruiz (1988) have investigated the natural convective heat transfer in convergent and divergent channels, both by experiments and by numerical solutions, for a limited range of parameters (inclination angle ranged from 0° to 15°), using water as fluid. For air, Kihm et al. (1993) reported experimental results of Nusselt number for converging channel by non-intrusively measuring the wall temperature gradients, using a laser specklegram technique for a limited number of convergence angles. Said (1996) and Shalash et al. (1997) have developed new investigations for convergent vertical channels. A comparison among these works and their ranges of application have been presented in Table 1. Some discrepancies and certain gaps in the ranges of the parameters considered have been detected.

This paper describes a numerical investigation of the natural buoyancy-driven fluid flow and the heat transfer in a vertical convergent channel. The present study was undertaken to examine the effects of converging angle for different channel aspect ratios, symmetric and asymmetric heating conditions and for a wide range of modified Rayleigh numbers, Ra^*. The working fluid was air. Since specific heat transfer correlations for the whole application range need to be provided in order to obtain a full understanding of these kind of systems, the main objective became for the research to obtain the local and average Nusselt numbers along the wall studying the

Table 1
Comparison among different studies of natural convection in converging channels

	Sparrow et al. (1988)	Kihm et al. (1993)	Said (1996)	Shalash et al. (1997)	This work
Ra^*	4×10^3–7×10^4	1–1×10^8	1–2×10^4	6.4–4.8×10^2	1–1×10^6
γ	0, 2, 5, 10, 15	0, 15, 30, 45, 60	0, 2, 5, 10	0, 2, 4, 8	0, 1, 2, 3, 6, 9, 12, 15, 30, 45, 60
Inter-plate spacing	(b_{max})	(b)	(b_{max})	($b' = b/2$)	(b)
b/L	1/11.4, 1/22.9	0.07, 0.1, 0.3, 0.35, 0.4	–	2/12, 2/17, 2/24	0.02, 0.05, 0.1, 0.2, 0.3, 0.4, 1, 2
Pr	5	0.71	0.72	0.7	0.71
Type of study	Numerical and experimental	Experimental	Numerical	Numerical and experimental	Numerical
Correlation	$Nu = 0.74[(b_{max}/L)Ra]^{0.24}$	None	None	$Nu = c(Ra^*)^m$ (based on b') (γ, c, m): (0°, 0.41, 0.38) (2°, 0.43, 0.33) (4°, 0.48, 0.29) (8°, 0.49, 0.28)	Sections 4.3 and 4.4

influence of the parameters aforementioned. In particular, symmetric heating condition has received more attention. The flow has been assessed using the general-purpose Fluent and Phoenics codes, both based on a finite volume procedure. As it could be expected, the computational results obtained were almost coincidental.

2. Governing equations and boundary conditions

Two alternatives could be employed to solve numerical problems of natural convection by commercial codes, as Fluent and Phoenics: variation of properties and Boussinesq approximation. When properties variation (variation of density, conductivity and viscosity) are considered, the full governing Navier–Stokes equations are solved. However, when the temperature variations are not so high, the Boussinesq approximation could be employed, and the thermophysical quantities are all assumed to be constant except for the density in the buoyancy force term. In this case, the system of equations may be simplified. In this paper, both alternatives have been employed. The first alternative has been used in Sections 4.1 and 4.2, and the second one in Sections 4.3 and 4.4.

Taking into account this fact, the results presented in this text may be divided into two parts. The first part (Sections 4.1, 4.2) contains the comparison of these results with those proposed in the bibliography. This step lets us to validate the numerical procedure employed. In this part we solve numerically the full equations considering the variation of properties in order to be able to reproduce the same parameters that those employed in the bibliography studied (see Zamora and Hernández, 1997). In order to close these full governing equations set, it is necessary to introduce the temperature dependence law of the viscosity and the conductivity of air (with T in kelvin),

$$\frac{\mu}{\mu_\infty} = \left(\frac{T}{T_\infty}\right)^{3/2} \frac{T_\infty + 110.6}{T + 110.6}, \qquad \frac{\kappa}{\kappa_\infty} = \left(\frac{T}{T_\infty}\right)^{3/2} \frac{T_\infty + 202.2}{T + 202.2}, \tag{1}$$

based on the well-known correlation of Sutherland, and those proposed by Sparrow and Gregg (1958), respectively. Neglecting pressure variations in the state equation, the perfect gas assumption leads to $\rho/\rho_\infty = T_\infty/T$. Specific heat at constant pressure remains mainly constant; thus, $c_p = c_{p,\infty}$ can be considered.

In the second part of the presented results (Sections 4.3, 4.4), a correlation is obtained using the Boussinesq approximation. For low enough values of the heating parameter $(T_w - T_\infty)/T_\infty$, constant thermophysical properties can be assumed for the fluid. Indeed, using the Boussinesq approximation to account for density variations in the buoyancy term in the vertical momentum equation, the two-dimensional form of conservation equations governing the fluid flow in a channel can be simplified significantly. Thus, the steady simplified-elliptic two-dimensional form of the conservation equations for the fluid flow in the channel formulated for x, y cartesian coordinates of Fig. 1 is (see Hernández et al., 1994):

$$\frac{\partial u}{\partial x} + \frac{\partial v}{\partial y} = 0, \tag{2}$$

$$\rho\left(u\frac{\partial u}{\partial x} + v\frac{\partial u}{\partial y}\right) = -\frac{\partial p'}{\partial x} + \beta\rho g(T - T_\infty) + \mu\left(\frac{\partial^2 u}{\partial x^2} + \frac{\partial^2 u}{\partial y^2}\right), \tag{3}$$

$$\rho\left(u\frac{\partial v}{\partial x} + v\frac{\partial v}{\partial y}\right) = -\frac{\partial p'}{\partial y} + \mu\left(\frac{\partial^2 v}{\partial x^2} + \frac{\partial^2 v}{\partial y^2}\right), \tag{4}$$

$$\rho c_p\left(u\frac{\partial T}{\partial x} + v\frac{\partial T}{\partial y}\right) = k\left(\frac{\partial^2 T}{\partial x^2} + \frac{\partial^2 T}{\partial y^2}\right), \tag{5}$$

where u and v are the velocity components in x and y directions; T the temperature; p' the reduced pressure, difference between the pressure p and the ambient pressure p_∞ given by the hydrostatic law $\mathrm{d}p_\infty/\mathrm{d}x = -g\rho_\infty$; β the coefficient of thermal expansion, equal to $1/T_\infty$ (with T in kelvin) for a perfect gas.

A schematic diagram of the channel assembly is presented in Fig. 1, wherein γ is the half angle of convergence, L the streamwise length of wall, and b the minimum inter-plate spacing, at the outlet of the channel. AB is the inlet section and CD the outlet section. The ratio between b and L is the channel aspect ratio.

The boundary conditions required for the present problem, imposed for both codes Fluent and Phoenics in a similar way, will now be described. Non-slip

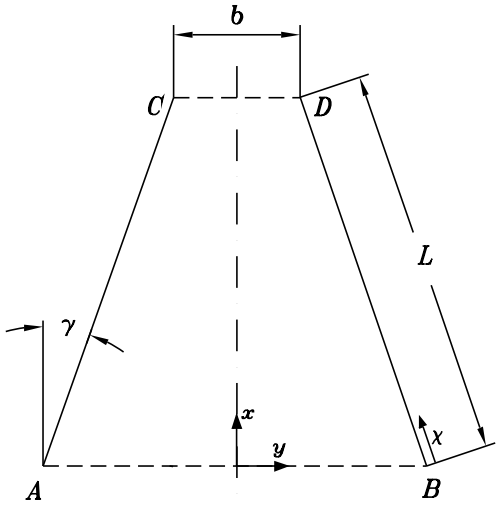

Fig. 1. Configuration of the computational domain.

conditions are imposed at the channel walls. At heated isothermal walls, $T = T_w$. At adiabatic walls, the heat flux from wall to fluid is zero. At the outlet section, the pressure defect is $p' = 0$ (pressure is the ambient pressure at exit), and the streamwise variations of velocity components and temperature are neglected. It might be expected that the effects of including an additional domain at the channel exit, so as to impose the boundary condition for pressure far enough, were not very important. At the inlet section, a total pressure (the sum of dynamic pressure and static pressure) of zero is imposed. In this way, it is assumed that Bernouilli equation holds at the entrance region outside the channel (indeed, the mass flow rate depends on the square root of pressure defect p'), and the streamwise variations of temperature are neglected. Under certain conditions, conduction effects at inlet could be important. It depends on the modified Rayleigh number, the aspect ratio and the domain considered. For example, for aspect ratios lower than 0.02 the conduction effects begin to be important for Rayleigh numbers lower than 1, for a certain geometry of the extended domain (Hernández et al., 1994). In these cases, an extended computational domain at inlet is required, as pointed out Martin et al. (1991). Influence of channel aspect ratio and inlet domain size has been studied by Hernández et al. (1994), and Zamora and Hernández (2001). A wider discussion about other boundary conditions in processes of natural convection in channels may be found in Desrayaud and Fichera (2002).

In a two-dimensional channel formed by two plates, it is well known that, for a given configuration and assuming fluid constant properties and Boussinesq approximation, the solution of governing equations in general depends on modified Rayleigh number based on minimum inter-plate spacing, $Ra^* = Ra(b/L)$, Prandtl number Pr and channel aspect ratio b/L. For channels with sloped walls, the inclination angle γ should be also considered. In addition, for variable properties, the solution depends on heating parameter $(T_w - T_\infty)/T_\infty$, and on the functions expressing the variation of thermophysical properties. In this work, some results of a systematic study of vertical converging channel with symmetric and asymmetric heating are presented. We have considered ranges of $4 \times 10^{-3} \leqslant Ra^* \leqslant 4 \times 10^6$, $0.02 \leqslant b/L \leqslant 2$ and $0 \leqslant \gamma \leqslant 60°$. For cases with constant properties, a fixed value of $Pr = 0.71$ (air) has been considered. When temperature variation properties have been retained, numerical results have been obtained for $(T_w - T_\infty)/T_\infty = 0.11$.

3. Numerical model

Results presented in this work have been obtained by using both the general-purpose Fluent and Phoenics codes, based on a finite volume procedures. In Fluent, the equations are discretized on a staggered grid (Patankar, 1980), using the 'Presto' scheme, which is similar to the staggered-grid scheme, with structured meshes employed in Phoenics, with a second-order upwind scheme for the convective terms. The Simple algorithm (Patankar and Spalding, 1972) is employed to solve the coupling between continuity and momentum equations through pressure (in Phoenics, the Simplest algorithm, which is a modified version of the Simple algorithm, is employed). In Phoenics, the results have been achieved employing a second-order differencing scheme of 'Muscl' type for the convective terms (Van Leer, 1979). The convergence criterion in each case was $(\phi^{i+1} - \phi^i)/\phi^i \leqslant 10^{-5}$, where i denotes iteration number and ϕ can stand for any of the dependent variables.

A structured, non-uniform mesh has been built in both codes. In order to ensure the accuracy of the numerical results, a grid dependence study was performed. For both the horizontal and vertical direction, and for each grid and aspect ratio an exponential law was used to obtain a fine grid near walls, inlet and outlet of the channel. Different ratios between number of cells in the vertical and horizontal directions were tested for each case solved (8/6 to 9/4). Important parameters such as average Nusselt number, which will be defined later, were compared and calculated at several grid resolution. The grids for the results reported in this paper were chosen for the change in average Nusselt number for each tested number of cells ratio to be low enough. As an example, for $Ra^* = 10^3$, $b/L = 0.1$ and $\gamma = 12°$, the chosen grid had (80×60) cells due to the fact that it ensures the lowest number of cells getting the required condition (see Table 2). For $Ra^* \geqslant 10^3$, influence of the

Table 2
Average Nusselt number for different grids, for $Ra^* = 10^3$, $b/L = 0.1$ and $\gamma = 12°$ (results obtained with Fluent)

V/H = 8/6	*Nu*	V/H = 9/5	*Nu*	V/H = 9/6	*Nu*	V/H = 9/4	*Nu*
8×6	2.83141	9×5	2.69538	9×6	2.83821	9×4	2.32227
16×12	3.21408	18×10	3.19656	18×12	3.21371	18×8	3.08762
32×24	3.12705	36×20	3.14976	36×24	3.12632	36×16	3.19979
64×48	3.02335	72×40	3.03520	72×48	3.02290	72×32	3.07456
80×60	2.98822	90×50	2.99925	90×60	2.98810	90×40	3.01943
128×96	2.98453	144×80	2.98802	144×96	2.98428	144×64	3.00117
160×120	2.96920	–	–	–	–	288×128	2.97767

V/H = number of cells in vertical/horizontal directions ratio.

grid was similar to that showed in Table 2; for $Ra < 10^3$, influence decreases and becomes insignificant. Most computations were carried out using this typical grid. In order to verify that the grid resolutions based on this criterion were adequate for resolving local quantities, additional grid studies were performed for each one of the cases included in this study. Although it is not shown in this paper, the local values of Nusselt number and the velocity values are observed to converge on one profile as the grid is refined.

Despite the fact that the numerical results obtained for average Nusselt number using a second order scheme as Muscl (Phoenics) or a second order upwind scheme (Fluent) are slightly higher than those obtained with a first-second order hybrid scheme (Phoenics) or a first order upwind scheme (Fluent), we assumed, for the problem studied in this work, that those discrepancies are negligible from a practical point of view (less than 5% for $Ra^* \leqslant 10^5$ and $\gamma \leqslant 15°$ in Phoenics, and less than 2% in Fluent).

4. Discussion of results

4.1. Isothermal parallel channel

In order to validate our numerical results with those obtained by Kihm et al. (1993), we analyzed a vertical–parallel channel ($\gamma = 0$) as a first step. In general, the numerical results obtained in this work have a reasonable agreement with experimental results of Kihm et al. (1993), as it can be observed in Fig. 2 (for local Nusselt number) and Fig. 3 (for average Nusselt number). These authors have explained that for $b/L = 0.05$ the local Nusselt number along the wall ($Nu_\chi = h\chi/\kappa$, where h is the heat transfer coefficient) started to deviate from the theory of Ostrach (1952) for a vertical isothermal plate,

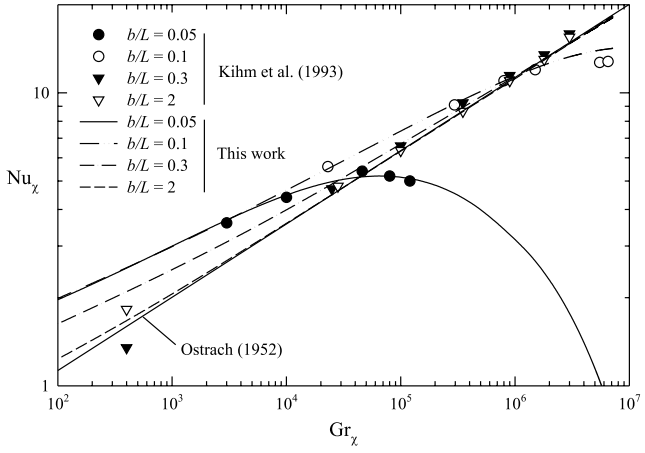

Fig. 2. Local Nusselt number versus local Grashof number for an isothermal parallel channel ($\gamma = 0$). Numerical model taking into account variable properties, for $(T_w - T_\infty)/T_\infty = 0.11$.

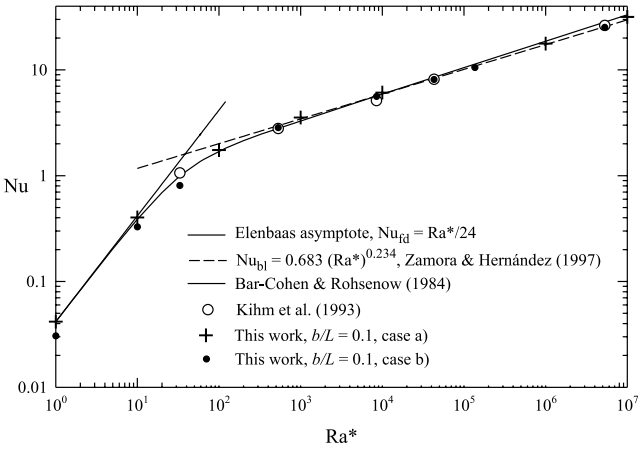

Fig. 3. Average Nusselt number as a function of modified Rayleigh number for an isothermal parallel channel ($\gamma = 0$). Numerical results obtained as follows: (case a) constant properties and Boussinesq approximation; (case b) variable properties for $(T_w - T_\infty)/T_\infty = 0.11$.

$$Nu_\chi = 0.5046(Gr_\chi/4)^{1/4}, \tag{6}$$

when local Grashof number $Gr_\chi = g\beta(T_w - T_\infty)\chi^3/\nu_r^2$ was larger than 5×10^4. This fact may be also appreciated in the numerical results of this work. As it can be seen in Fig. 2, for a channel aspect ratio of $b/L = 0.05$, very good agreement is observed between numerical and experimental results for Nu_χ. The deviation from single plate theory can be justified by considering that the two thermal boundary layers start interfering with each other, what leads to a decrease in the heat transfer for $Gr_\chi > 5 \times 10^4$. Notice that Kihm et al. (1993) based their exposure of results on ν_r, at T_r given from Sparrow and Gregg (1958), $T_r = T_w - 0.38(T_w - T_\infty)$.

The data obtained by Kihm et al. (1993) for average Nusselt number, defined as

$$Nu = \frac{1}{L}\int_0^L Nu_\chi \, d\chi, \tag{7}$$

have a very good agreement with correlations of literature (Bar-Cohen and Rohsenow, 1984; Elenbaas, 1942; Zamora and Hernández, 1997) in the case of parallel channel ($\gamma = 0$). However, experimental results (Kihm et al., 1993) showed in Fig. 3 have been obtained varying the inter-plate spacing; in fact, it is only valid for Ra^* high enough, for which upstream heat conduction is negligible (see papers of Martin et al., 1991, and Hernández et al., 1994). The numerical results of the present work for a channel aspect ratio $b/L = 0.1$ fit very well with experimental results of Kihm et al. (1993).

4.2. Isothermal converging channel

For converging channel ($\gamma > 0$), the gravity must be reduced through ($\cos\gamma$) in non-dimensional parameters, as it will be explained later. Local Nusselt numbers

obtained in this work have been compared with those proposed by Kihm et al. (1993). Fig. 4 is equivalent to Fig. 2, but for converging channel ($\gamma = 30°$). An appreciable disagreement can be observed between the results showed in this figure, though the trends of curves are the same. For high channel aspect ratio, the results fit the Ostrach (1952) theory. When b/L decreases, local Nusselt number becomes detached from Ostrach curve and tends to decay. The physical reason for this behavior is that, for converging channel, the thermal boundary layers started interfering with each other when the channel aspect ratio was low enough, for a given local Grashof number. Therefore, a strong diminution of heat transfer between walls and the fluid occurs. The following increase of local Nusselt number near the top opening that Kihm et al. (1993) have measured, has been reproduced in this work numerically. We have observed that, for $\gamma > 0$, the more thermal boundary layers of both plates interfere with each other, the more they tend to narrow at the top opening (see Fig. 5). This flow pattern forces the local heat transfer to increase dramatically between the emerging flow stream and cooler ambient air situated above. Although numerical and experimental data show a similar trend, certain differences between the values of both results have been found (see Fig. 6). New computations including an outlet region in the channel seem to be necessary to understand these differences.

Results obtained in this work of average Nusselt number for converging channels have been compared with those proposed by Said (1996), Shalash et al. (1997), Sparrow et al. (1988) and Kihm et al. (1993). This comparison may be appreciated in Table 1 and Figs. 6, 7. In the fully developed region, all the data show the variation of Nusselt number with the angle of convergence but there are some differences between the results presented by the different authors.

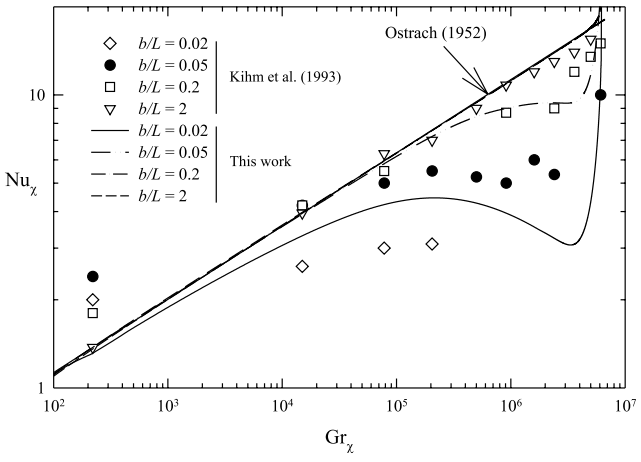

Fig. 4. Local Nusselt number versus local Grashof number for an isothermal converging channel with $\gamma = 30°$. Numerical model with variable properties for $(T_w - T_\infty)/T_\infty = 0.11$.

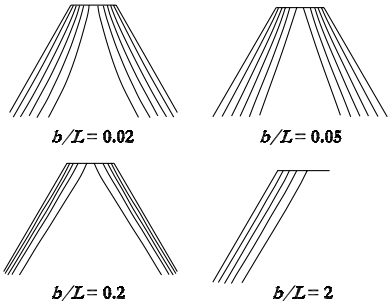

Fig. 5. Isothermal lines obtained at the outlet of the converging channel ($\gamma = 30°$) for different aspect ratios (figures have been scaled).

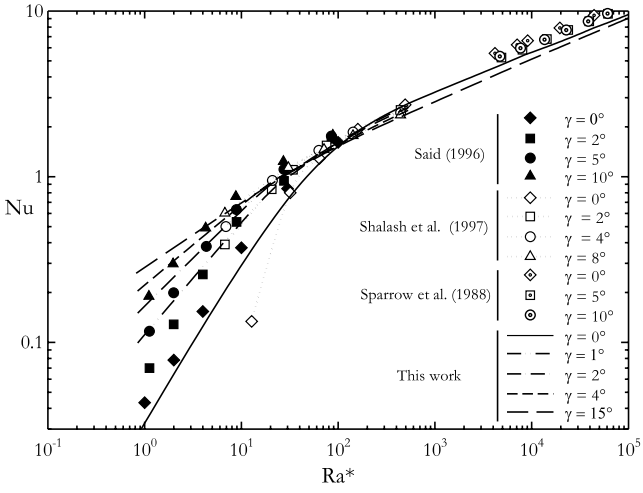

Fig. 6. Comparison among different studies of natural convection in converging channels of the average Nusselt number as a function of modified Rayleigh number for different angles of convergence. Numerical model taking into account variable properties, for $(T_w - T_\infty)/T_\infty = 0.11$.

Shalash et al. (1997) used a Mach–Zehnder interferometer to obtain heat transfer coefficients for $\gamma = 0°$, 2°, 4° and 8° and $b/L = 2/12$, 2/17 and 2/24; their numerical and experimental results showed an excellent agreement. The investigations of these authors have been based on minimum inter-plate spacing, but differences of 10% for modified Rayleigh numbers lower than 10 between the results presented in this work and those proposed by these authors were obtained. They proposed atypical values of Nusselt number for $\gamma = 0$ in fully developed regime. These differences may be appreciated in Fig. 6.

Sparrow et al. (1988) studied numerically and experimentally the influence of the angle of convergence for the boundary layer regime. They found that the merging of results for cases with $\gamma > 0$ into those obtained for a vertical parallel channel ($\gamma = 0$) was best accomplished by the use of maximum inter-plate space, finding deviations between the corresponding convergent-channel and parallel-channel average Nusselt numbers to about 5%. They employed water as fluid. These results and

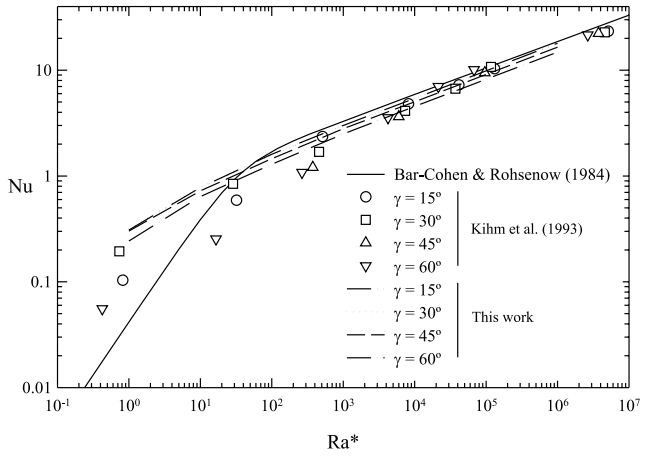

Fig. 7. Average Nusselt number as a function of modified Rayleigh number for an isothermal converging channel. Numerical model with variable properties for $(T_w - T_\infty)/T_\infty = 0.11$.

those proposed in this work show the same trend. In spite of that, certain differences due to the Prandtl number considered in both cases have been detected.

Said (1996) obtained numerical data by a code based on finite elements. Our results show a similar stratification to those proposed by this author, but with some differences, probably due to the differences in the codes employed. These differences have been shown in Fig. 6. He found that merging was best achieved by maximum inter-plate spacing, even for low modified Rayleigh numbers ($1 < Ra^* < 2 \times 10^2$).

In the work presented, for a more wide range of modified Rayleigh numbers, it has been found that it is more appropriate to use the minimum inter-plate spacing, according to Kihm et al. (1993). As it has been shown in the previous section, a very good agreement with correlations for vertical parallel channels is reached if the results for average Nusselt number versus modified Rayleigh number obtained are based on the opening at the top of the channel, b. This outlet opening means the physical exit section for the flow of fluid.

Kihm et al. (1993) proposed experimental results for a wide range of the modified Rayleigh number. Significant differences were appreciated between these results and those proposed in this work, particularly for low Ra^*, though the general trend is good (see Fig. 7 and Table 3).

4.3. Correlation for average Nusselt number in isothermal converging channel

Since our aim is to obtain a correlation for average Nusselt number at heated walls, from now on, all

Table 3
Average Nusselt number Nu_L, for Gr_L (based on v_r) ranged from 3.58×10^6 ($\gamma = 60°$) to 7.16×10^8 ($\gamma = 0$)

b/L	$\gamma = 0°$	$\gamma = 15°$	$\gamma = 30°$	$\gamma = 45°$	$\gamma = 60°$	
0.02	1.382	13.08	12.87	11.32	9.213	(Fluent)
	–	5.170	9.720	–	2.780	(Kihm)
	1.454	15.57	16.87	16.01	–	(Phoenics)
0.05	15.65	21.19	20.31	18.40	15.64	(Fluent)
	21.21	11.80	16.88	–	5.080	(Kihm)
	16.10	21.93	21.72	20.58	–	(Phoenics)
0.1	27.65	23.84	22.86	21.19	18.77	(Fluent)
	27.87	23.55	16.93	12.06	10.80	(Kihm)
	27.90	24.04	23.33	22.18	–	(Phoenics)
0.2	27.21	24.37	23.33	21.86	19.21	(Fluent)
	25.65	24.01	20.67	18.19	17.75	(Kihm)
	27.41	24.56	23.74	22.54	–	(Phoenics)
0.3	26.24	24.29	23.35	21.84	19.97	(Fluent)
	27.12	24.17	22.31	–	23.37	(Kihm)
	26.31	24.57	23.81	22.66	–	(Phoenics)
0.4	25.57	24.21	23.31	21.74	19.67	(Fluent)
	–	25.82	26.86	23.64	25.25	(Kihm)
	25.60	24.52	23.86	22.73	–	(Phoenics)
1.0	24.46	23.98	23.29	21.70	19.51	(Fluent)
	26.26	23.35	22.79	22.28	21.53	(Kihm)
	24.67	24.53	23.98	23.11	–	(Phoenics)
2.0	24.24	23.90	23.24	21.68	19.36	(Fluent)
	–	25.93	23.03	22.44	20.91	(Kihm)
	24.83	24.61	24.26	23.51	–	(Phoenics)
Ostrach (1952)	24.95	24.74	24.07	22.88	20.98	

In each cell, first results obtained with Fluent appear, second, those obtained by Kihm et al. (1993), and third those obtained with Phoenics.

numerical results presented were obtained by using the constant properties model for fluid, with Boussinesq approximation for body force term. In this way, it is possible to remove the influence of heating parameter, $(T_w - T_\infty)/T_\infty$.

Although Sparrow et al. (1988), and Sparrow and Ruiz (1988) were able to correlate two-dimensional heat transfer results on a converging channel in terms of maximum inter-plate spacing, similar attempts to correlate the channel data of this study were unsuccessful. In a converging channel, the buoyancy force is no longer exclusively in the streamwise direction since a component also exists perpendicular to the heated surface. Thus, the specific buoyancy force that accelerates the fluid in the thermal boundary layer is $(g\beta\Delta T\cos\gamma)$ instead of $(g\beta\Delta T)$. For this reason, the $(\cos\gamma)$ correction was applied to the modified Rayleigh number definition. The use of Ra^* based on $(\cos\gamma)$ factor represents the assumption of an already widely used practice for inclined plates, corroborated for inclined channels by Straatman et al. (1994). On the other hand, the Nusselt number is also influenced by the angle of convergence. The relative separation between the plates that form the channel may be modified by changing the angle of convergence, and so the heat transfer produced in this configuration is affected. The definition of Ra^* as $(Pr)(b/L)g\beta\Delta T(\cos\gamma)b^3/v_\infty^2$ leads to the results for convergent channel in agreement with those obtained for a parallel channel in the boundary-layer regime (for $Ra^* \geqslant 10^3$ approximation).

With regards to inter-plate spacing, as mentioned above, correlation of our numerical results was best achieved by minimum inter-plate spacing b. From our point of view, results based on b seem to be more coherent with the criterion employed in parallel vertical channels in the literature. When the results are based on b_{max}, there are some aspect ratios that physically cannot be reproduced, due to the convergence of the channel. The value for b_{max} to obtain a channel with an open exit should be bigger than $(2L_p\sin\gamma)$. When b_{max} is lower than this value both plates interacts and a channel without exit is obtained. Thus, it is not possible to get a set of cases based on maximum inter-plate spacing that was equivalent to those constructed with minimum inter-plate spacing, for a fixed channel aspect ratio. In Fig. 8, both modified Rayleigh and Nusselt numbers are based on b_{max}. For $b_{max}/L = 0.5$, it was necessary to fix $b/L = 0.395$, 0.290, 0.187 and 0.084 for $\gamma = 3°$, 6°, 9° and 12°, respectively. In this way, the transition between fully developed regime and boundary-layer regime strongly depends on the angle of convergence, and merging of results was obtained for unreasonably high Ra^* (a fully developed regime for $Ra^* \geqslant 10^3$ and high values of γ could be obtained). This behavior does not occur if relevant dimensionless parameters are based on b, as it can be seen in Fig. 9. The convergence obtained

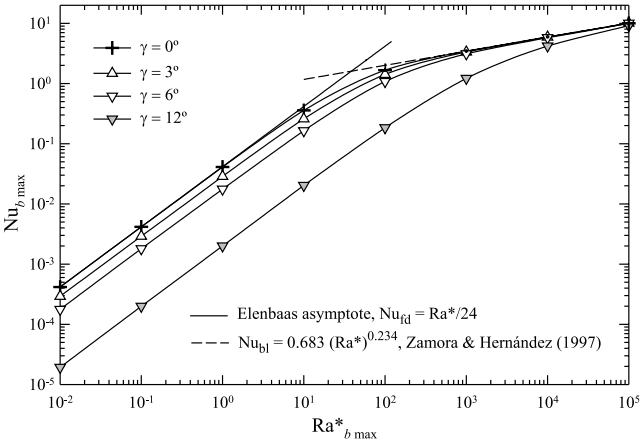

Fig. 8. Average Nusselt number as a function of modified Rayleigh number, both based on b_{max}, for $b_{max}/L = 0.5$. Constant properties and Boussinesq approximation.

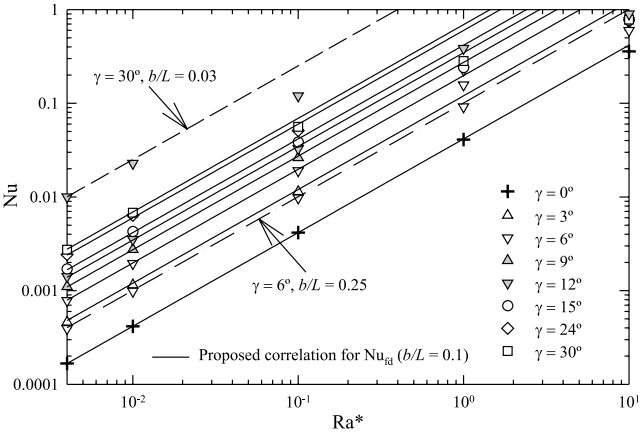

Fig. 9. Fully developed Nusselt number versus modified Rayleigh number, for $b/L = 0.1$. Constant properties and Boussinesq approximation.

by Said (1996) between cases based on b_{max} and those based on b, might be explained by the fact of not having kept the channel aspect ratio constant.

According to the numerical results presented in this paper, a correlation was determined both for fully developed (fd) regime and for boundary-layer (bl) regime, using the general expression suggested by Churchill and Usagi (1972). The form of this blended relation for average Nusselt number is expressed as

$$Nu = \left[Nu_{fd}^n + Nu_{bl}^n\right]^{1/n}. \tag{8}$$

It can be observed in Fig. 9 that numerical results do not follow the same asymptotic fully developed behavior at low Ra^* for different values of γ. With dimensionless governing parameters based on minimum inter-plate spacing, average Nusselt number increases as well as converging angle does, for a low enough Ra^*. The reason for that might by in the augmentation of fluid vol-

ume under buoyancy force, in which case an asymptotic correlation for fully developed regime can be obtained by the assumption of differential body forces over the flow field. Into core region of the domain, the buoyance force is $(g\beta\Delta T)(bL\cos\gamma)$, and within the rest of the domain, at both lateral triangles, it is $(g\cos\gamma\beta\Delta T)(L^2\sin\gamma\cos\gamma)(\Lambda)$, where Λ takes into account the non-uniformity of specific body force $(g\cos\gamma\beta\Delta T)$ in those flow fields, and likewise the weighting of sizes of the two zones. So, the relative increase of buoyancy force with respect to a vertical parallel channel of $b\times L$ dimensions is

$$\cos\gamma\left[1+\Lambda\frac{(\sin\gamma)(\cos\gamma)}{b/L}\right]. \tag{9}$$

Assuming that this quantity leads to the average Nusselt number increasing with respect to those that might be obtained for the above reference channel, and including $(\cos\gamma)$ in the modified Rayleigh number definition, as pointed out before, we obtain

$$Nu_{\mathrm{fd}}=\frac{Ra^*}{24}\left[1+\Lambda\frac{(\sin\gamma)(\cos\gamma)}{b/L}\right], \tag{10}$$

valid for both low enough Ra^* and γ. It should be remarked that the use of Eq. (10) implies the assumption of fully developed flow; indeed, the pressure drop should be balanced by buoyancy effects. Then, the above augmentation of buoyancy force is mainly balanced by the convective term $\rho u(\partial u/\partial x)$, which appears as a result of streamwise cross section variation when $\gamma>0$. This behavior has been confirmed by comparison of quantities obtained in the numerical simulation for $Ra^*=0.004$ and 0.01.

For modified Rayleigh numbers aforenamed, $b/L=0.03$, 0.1 and 0.25, and $0\leqslant\gamma\leqslant30°$, results obtained for average Nusselt number follow closely Eq. (10) with values $\Lambda=4.15$, 3.60 and 3.40. Once that $\gamma>0$, disagreement increases as well as b/L decreases and γ increases; however, the maximum deviation was about 5% for $Ra^*\leqslant0.01$. As it might be expected, Λ was roughly constant, but since a significant increase for the lowest channel aspect ratio was reached, supplementary computations for additional channel aspect ratios were carried out. As a result, the following correlation:

$$\Lambda=3.2-0.027\ln(b/L)+0.071[\ln(b/L)]^2 \tag{11}$$

takes into account the slight dependence with respect to b/L with a deviation less than 1% for $0.03\leqslant b/L\leqslant0.25$.

In this first part of the correlation, the influence of the channel aspect ratio may also be appreciated, for angles of convergence different from zero. Most of the results of Fig. 9 corresponds to $b/L=0.1$, but in order to show the validity of the proposed correlation, cases with different aspect ratio have also been drawn. Notice that when $\gamma\to0$, Eq. (10) may be reduced to $Nu_{\mathrm{fd}}=Ra^*/24$, which represents the fully developed limit determined by Elenbaas (1942) for isothermal vertical channels. When $\gamma>0$, for both constant channel aspect ratio and modified Rayleigh number, the heated volume within the channel increases, and as a consequence of that, the buoyancy effect also increases and causes a bigger mass flow rate in the channel than corresponding to cases with $\gamma=0$.

On the other hand, the boundary-layer expression for average Nusselt number takes the form

$$Nu_{\mathrm{bl}}=\mathscr{A}(Ra^*)^{\mathscr{B}}, \tag{12}$$

valid for $Ra\geqslant10^3$, which indicates flow characteristics approaching the isolate-plate (or boundary-layer) regime. The numerical results can be correlated for $b/L=0.1$ (see Fig. 10), with a maximum error of around 1.5% in the range $10^3\leqslant Ra^*\leqslant10^6$, with the following expressions for $\mathscr{A}$ and $\mathscr{B}$:

$$\begin{aligned}\mathscr{A}&=0.693\left[1-0.380(\sin\gamma)^{1/4}\right];\\ \mathscr{B}&=0.234\left[1+0.214(\sin\gamma)^{1/2}\right].\end{aligned} \tag{13}$$

When $\gamma\to0$, then $Nu_{\mathrm{bl}}=0.693(Ra^*)^{0.234}$ (Zamora and Hernández, 2001, obtained $Nu_{\mathrm{bl}}=0.614(Ra^*)^{0.236}$). In order to simplify, the influences of the channel aspect ratio on $\mathscr{A}$ and $\mathscr{B}$ were neglected. With values of $\mathscr{A}$ and $\mathscr{B}$ given by (13), the proposed boundary-layer asymptote also follows the numerical results for alternative values of $b/L=0.03$ and 0.25, but with a deviation slightly higher than those reached for $b/L=0.01$: maximum error of 4.5% for $10^3\leqslant Ra^*\leqslant10^5$ and 7.5% for $Ra^*=10^6$.

The value of the exponent n was obtained by correlating the numerical results presented in this work. This coefficient, as a function of b/L and γ, may be determined by

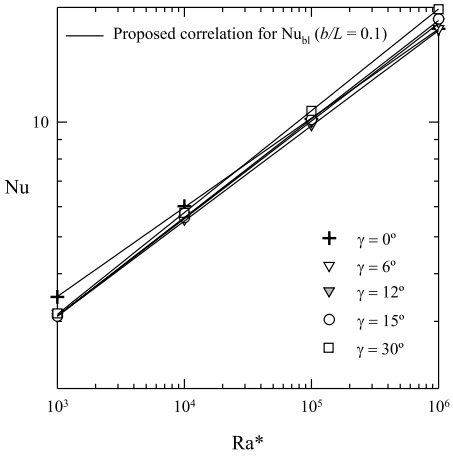

Fig. 10. Boundary-layer Nusselt number versus modified Rayleigh number, for $b/L=0.1$. Constant properties and Boussinesq approximation.

$$n = -\frac{1}{6}\left[9.0 - \frac{(\sin\gamma)^{1/3}}{0.14 + (b/L)}\right]. \tag{14}$$

On the other hand, the numerically determined Nusselt numbers were compared with those predicted by Eq. (8) (see Fig. 11 for $b/L = 0.1$, and Fig. 12 for $b/L = 0.25$, both for symmetric heating conditions), with agreement in the 0–5% range and averaged error of 2% for $4 \times 10^{-3} \leqslant Ra^* \leqslant 10^6$, $b/L = 0.1$ and $0 \leqslant \gamma \leqslant 30°$. Obviously, best agreement was just reached for $b/L = 0.1$. Nevertheless, the proposed correlation also follows the present numerical results satisfactorily for $b/L = 0.03$ and $b/L = 0.25$ (the same maximum deviation than those aforementioned in the boundary-layer regime were reached). In general, differences increase between results obtained for Nusselt number for a parallel channel and for a converging channel, and so does the inclination angle. But note that for a low enough Ra^*, major Nusselt number appears for $\gamma = 30°$, whereas for a high enough Ra^*, major Nu inversely corresponds to $\gamma = 0$ ($Ra^* = 10^3$ in Fig. 10, for example). The change of trend occurs at the transition from fully developed to boundary-layer regimes, though for $Ra^* \geqslant 10^5$ (see Fig. 10), the maximum average Nusselt number is for major γ again.

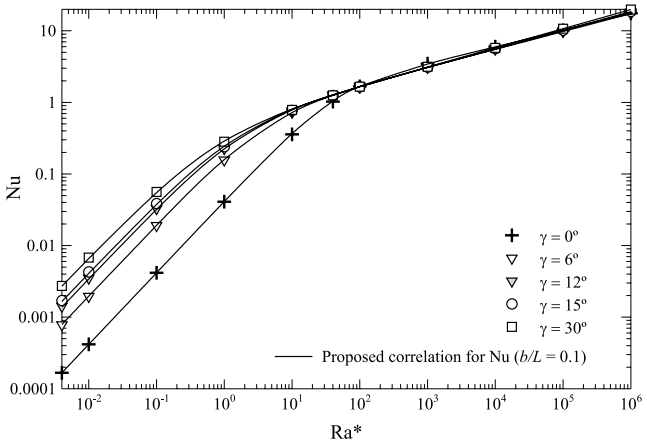

Fig. 11. Generalized correlation proposed for average Nusselt number. $b/L = 0.1$. Constant properties and Boussinesq approximation. Symmetric heating conditions.

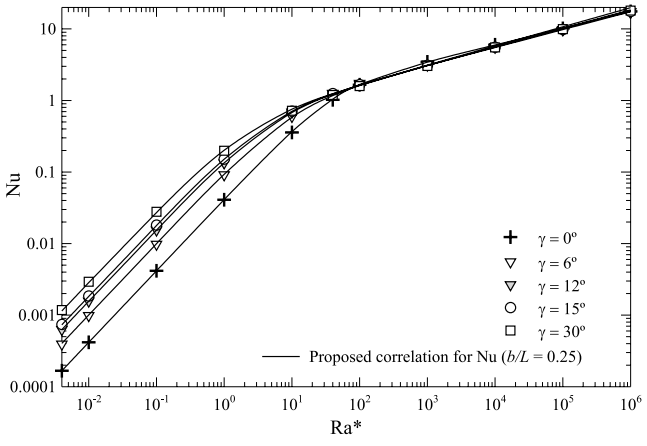

Fig. 12. Generalized correlation proposed for average Nusselt number. $b/L = 0.25$. Symmetric heating conditions.

According to Kihm et al. (1993), the average Nusselt number values obtained exceed those of the fully developed limit of parallel channel, as explained above. Physically, this may be due to the fact that the thermal boundary layers along the inclined walls are slighter than along the vertical wall, because the incoming core flow, which volume increases as well as γ does, as noted previously, compels the fluid near the sloped walls. This last trend decreases when Ra^* increases, therefore in the transition zone, the Nusselt numbers obtained for converging channel are smaller than those of vertical parallel plates, even if the gravity force is reduced at modified Rayleigh number through $(\cos\gamma)$. For large enough values of Ra^*, the difference tends to diminish, due to the similar way of thermal boundary layers developing for different converging angles. In the transition zone aforementioned, the thermal boundary layers merge near the top opening, whereas in the case of parallel channel this does not occur; this behavior leads to us obtain a smaller average Nusselt number for an intermediate range of modified Rayleigh numbers, though for very large values of Ra^* it is possible to find values of Nu larger than those corresponding to vertical parallel plates, as pointed out before.

4.4. Correlation for average Nusselt number in isothermal-adiabatic converging channel

In this work, attention is focused mainly on symmetric heating conditions. However, in order to check the validity of the proposed correlation for average Nusselt number, cases with asymmetrical heating (one isothermal plate and the other an adiabatic one) have also been solved for a channel aspect ratio equal to 0.1. Following a similar reasoning to those given in the previous section, it can be obtained that the fully developed regime correlation for Nu is

$$Nu_{\mathrm{fd}} = \frac{1}{12}\left[1 + \Lambda\frac{(\sin\gamma)(\cos\gamma)}{b/L}\right], \tag{15}$$

with $\Lambda = 3.6$, too. The corresponding values of $\mathscr{A}$ and $\mathscr{B}$ for Nu_{bl}, obtained by correlating numerical results for $b/L = 0.1$ are:

$$\begin{aligned}\mathscr{A} &= 0.631\left[1 - 0.317(\sin\gamma)^{1/3.5}\right];\\ \mathscr{B} &= 0.238\left[1 + 0.210(\sin\gamma)^{1/2.3}\right].\end{aligned} \tag{16}$$

Finally, the blended coefficient n can be calculated by

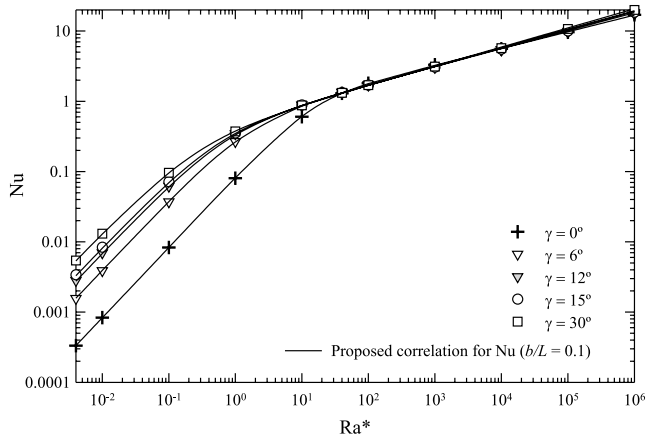

Fig. 13. Generalized correlation proposed for average Nusselt number. $b/L = 0.1$. Asymmetric heating conditions.

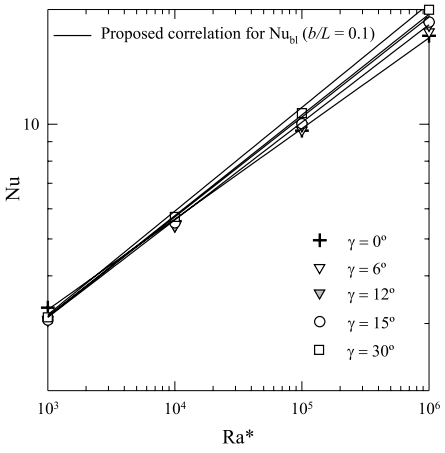

Fig. 14. Boundary-layer Nusselt number versus modified Rayleigh number, for $b/L = 0.1$. Asymmetric heating conditions.

$$n = -\frac{1}{6}\left[9.6 - \frac{(\sin\gamma)^{1/3}}{0.14 + (b/L)}\right]. \tag{17}$$

As illustrated in Fig. 13 (for $b/L = 0.1$, and asymmetric heating conditions), the present numerical results are in good agreement with the proposed correlation. A same agreement as those reached in symmetrically heated cases was obtained. Further inspection of results obtained reveals that average Nusselt number has slightly distinct trend, as a function of Ra^*, from those trends corresponding to cases with symmetrical heating for boundary-layer regime (see Fig. 14). In general, this behavior implies a very small difference, as it can be deduced from comparison of Eqs. (13) and (16).

5. Conclusions

The steady, laminar and elliptic numerical model developed in codes Fluent and Phoenics has been validated by the experimental results of Kihm et al. (1993) and other authors for natural buoyancy-driven flows in converging channels. Different aspects of the problem, such as the definition manner of the modified Rayleigh number and the influence of converging angle on local and average Nusselt numbers, have been studied. The following concluding remarks can be made:

1. Best correlation of results obtained for average Nusselt number was reached by using the modified Rayleigh number based on minimum inter-plate spacing.
2. To the best knowledge of the authors, there is no prior literature dealing with a generalized correlation for average Nusselt number in isothermal and isothermal-adiabatic converging channel. In the present work, a blended correlation has been reported, valid for the range $Ra^* \leqslant 10^6$ and $0 \leqslant \gamma \leqslant 30°$. It can be summarized for symmetrical heating as follows: the Nusselt number is given by (8), with (10) and (11) for fully developed asymptotic limit and with (12) and (13) for boundary-layer asymptotic limit; finally, the blended exponent is given by (14).
3. It has been found that both the converging angle and the channel aspect ratio take part in the asymptotic correlation for fully developed Nusselt number.

References

Bar-Cohen, A., Rohsenow, W.M., 1984. Thermally optimum spacing of vertical, natural convection cooled, parallel plates. J. Heat Transfer 106, 116–123.

Baskaya, S., Aktas, M.K., Onur, N., 1999. Numerical simulation of the effects of plate separation and inclination on heat transfer in buoyancy driven open channels. Int. J. Heat Mass Transfer 35, 273–280.

Bianco, N., Morrone, B., Nardini, B., Naso, V., 2000. Air natural convection between inclined parallel plates with uniform heat flux at the walls. Heat Technol. 18, 23–45.

Bodoia, J.R., Osterle, J.F., 1962. The development of free convection between heated vertical plates. J. Heat Transfer 84, 40–44.

Churchill, S.W., Usagi, J.F., 1972. A general expression for the correlation of rates of transfer and other phenomena. AIchE Y. 18, 1121–1128.

Desrayaud, G., Fichera, A., 2002. Laminar natural convection in a vertical isothermal channel with symmetric and surface-mounted rectangular ribs. Int. J. Heat Fluid Flow 23, 519–529.

Elenbaas, W., 1942. Heat dissipation of parallel plates by free convection. Physica 9 (1), 1–28.

Guo, Z.Y., Wu, X.B., 1993. Thermal drag and critical heat flux for natural convection of air in vertical parallel plates. J. Heat Transfer 124, 124–129.

Hernández, J., Zamora, B., Campo, A.,1994. On the effect of Prandtl number and aspect ratio upon laminar natural-convection flows in vertical channels. In: Hewitt, G.F. (Ed.), Proceedings of the Tenth International Heat Transfer Conference 5, Brighton, pp. 483–488.

Kihm, K.D., Kim, J.H., Fletcher, L.S, 1993. Investigation of natural convection heat transfer in converging channel flows using a specklegram technique. J. Heat Transfer 115, 140–148.

Manca, O., Morrone, B., Nardini, S., Naso, V., 2000. Natural convection in open channels. In: Sundén, B., Comini, G. (Eds.),

Computational Analysis of Convection Heat Transfer 7. WIT Press, Southampton, pp. 235–278.

Martin, L., Raithby, G.D., Yovanovich, M.M., 1991. On the low Rayleigh number asymptote for natural convection through an isothermal, parallel-plate channel. J. Heat Transfer 113, 899–905.

Ostrach, S., 1952. An analysis of laminar free convection heat transfer about a flat plate parallel to the direction of the generating body force. NACA TN-2635.

Patankar, S.V., 1980. Numerical Heat Transfer and Fluid Flow. Hemisphere, New York.

Patankar, S.V., Spalding, D.B., 1972. A calculation procedure for heat, mass and momentum transfer in three-dimensional parabolic flows. Int. J. Heat Mass Transfer 15, 1787–1806.

Said, S.A., 1996. Investigation of natural convection in convergent vertical channels. Int. J. Energy Research 20, 559–567.

Shalash, J.S., Tarasuk, J.D., Naylor, D., 1997. Experimental and numerical analysis of natural convection heat transfer in vertical converging channel flows. In: Giot, M., Mayinger, F., Celata, G.P. (Eds.), Proceedings of the Fourth Experimental Heat Transfer. Fluid Mechanics and Thermodynamics 4, pp. 2167–2174.

Sparrow, E.M., Gregg, J.L., 1958. The variable fluid property problem in free convection. J. Heat Transfer 80, 879–886.

Sparrow, E.M., Ruiz, R., 1988. Experiments on natural convection in divergent vertical channels and correlation of divergent, convergent, and parallel-channel Nusselt numbers. Int. J. Heat Mass Transfer 31, 2197–2205.

Sparrow, E.M., Ruiz, R., Azevedo, L.F.A., 1988. Experimental and numerical investigations of natural convection inconvergent vertical channels. Int. J. Heat Mass Transfer 31, 907–915.

Straatman, A.G., Naylor, D., Floryan, J.M., Tarasuk, J.D., 1994. A study of natural convection between inclined isothermal plates. J. Heat Transfer 116, 243–245.

Van Leer, B., 1979. Towards the ultimate conservative difference scheme V. A second order sequel to Gadunov's method. J. Comput. Phys. 32, 101–136.

Zamora, B., Hernández, J., 1997. Influence of variable properties effects on natural convection flows in asymmetrically-heated vertical channels. Int. Comm. Heat Mass Transfer 24, 1153–1162.

Zamora, B., Hernández, J., 2001. Influence of upstream conduction on the thermally optimum spacing of isothermal, natural convection-cooled vertical plate arrays. Int. Comm. Heat Mass Transfer 28, 201–210.